ELSEVIER

Physica B 279 (2000) 130–133

PHYSICA B

www.elsevier.com/locate/physb

Diffusing acoustic wave spectroscopy of fluidized suspensions

J.H. Page[a,*], M.L. Cowan[a], D.A. Weitz[b]

[a]*Department of Physics and Astronomy, University of Manitoba, Winnipeg, MB, Canada R3T 2N2*
[b]*Department of Physics and Astronomy, University of Pennsylvania, Philadelphia, PA 19104, USA*

Abstract

The velocity fluctuations and local strain rate in a fluidized suspension of particles are investigated using the new ultrasonic technique of diffusing acoustic wave spectroscopy. DAWS probes the relative motion of the particles at very short length scales down to the inter-particle separation, and allows the spatial correlations of the velocity fluctuations to be probed by varying the transport mean free path of the diffusing ultrasonic waves. Our results demonstrate the power of this ultrasonic technique to probe the dynamics of sedimenting particles at larger length scales and Reynolds numbers than can be achieved by light scattering methods.

Keywords: Diffusing acoustic wave spectroscopy; Multiple scattering of ultrasound; Sedimentation; Fluidized beds

The scattering of ultrasonic waves from objects embedded deep within optically opaque materials has enabled powerful imaging techniques to be developed for probing their properties, structure and dynamics. Examples range from the location cracks in airplane wings to the imaging of blood flow in human patients. These techniques rely on measurements of ultrasound that propagates directly, or ballistically, between a single scatterer and the generator/detector, thereby precluding the study of materials in which very strong multiple scattering of ultrasonic waves occurs. However, there are many cases where the incident acoustic waves are scattered many times from inhomogeneities in the material, motivating the development of new techniques for extracting information on the structure and dynamics of such materials. In this paper we describe one such technique, diffusing acoustic wave spectroscopy (DAWS), that provides a new method for investigating the motion of the scattering inhomogeneities by measuring the temporal fluctuations of multiply scattered sound. As in the analogous optical technique of diffusing wave spectroscopy [1,2], DAWS makes use of the diffusion approximation to describe the propagation of ultrasound through the material, an approximation that we have shown to be a powerful tool for successfully describing the multiple scattering of acoustic waves in strongly scattering media [3–5]. Extremely good spatial sensitivity is obtained through the use of multiply scattered waves, since each scatterer need move only a minute fraction of a wavelength for its motion to be detected.

We apply this technique to the study of fluidized suspensions of non-Brownian particles, where the fluid is flowed upwards to counterbalance the gravitational forces that would otherwise cause the particles to settle to the bottom of the container. Even though the ensemble average velocity of the particles is zero, they are far from stationary, and understanding how the particles move in fluidized suspensions is an important and challenging problem, whose solution has remained elusive. This problem is relevant not only to applications in chemical reactors where the stability of fluidized suspensions can be problematic, but also to fundamental studies of particle sedimentation, where conflicting theoretical predictions about a possible divergence of the velocity fluctuations with system size have been proposed [6,7]. Recent experiments [8] have helped to elucidate the behaviour in the limit of creeping flow or low particle Reynolds number $\mathrm{Re} = 2aV_0/\eta \sim 10^{-4}$, where a is the particle radius, V_0 is the Stokes settling velocity and η is the fluid viscosity. In these experiments it was found that the velocity fluctuations were correlated over remarkably

* Corresponding author. Tel.: +1-204-474-9852; fax: +1-204-474-7622.
E-mail address: jhpage@cc.umanitoba.ca (J.H. Page)

0921-4526/00/$ - see front matter
PII: S0921-4526(99)00698-5

long length scales, ξ, thereby offering a phenomenological explanation for how the divergence in the velocity fluctuations is cut off. However, the origin of this new length scale has not been resolved despite recent theoretical progress [9,10], and what happens to these velocity correlations as Re is increased has not been investigated. Unfortunately, higher Re are most easily attained with the use of larger particles, which precludes the use of light scattering methods that have been so successfully used at low Re to study the dynamics, since the relevant particle motion is so much larger than the wavelength λ of the probe light. Since ultrasonic wavelengths are much larger than optical ones, we show that DAWS has considerable potential to address these unanswered questions about the Re dependence of velocity fluctuations and correlations in fluidized suspensions.

To probe the behaviour at higher Re, we used a fluidized bed containing monodisperse glass beads suspended in a fluid mixture of glycerol and water. For the data presented here, the bead size and glycerol concentration were chosen so that Re ~ 0.3. The volume fraction of glass beads ϕ was varied between 0.2 and 0.5 by adjusting the flow rate V_{flow}. Measurements of V_{flow} allowed the ϕ-dependence of the average sedimentation velocity ($V_{\text{sed}} = V_{\text{flow}}$) to be determined as shown in Fig. 1, giving results in good agreement with the well-established semi-empirical relation [11] $V_{\text{sed}}/V_0 = (1-\phi)^{-K_2}$ where $K_2 = -4.4$ for our data.

The particle dynamics in the suspension were investigated using DAWS [12,13] by placing the fluidized bed in a water tank between a plane-wave generating transducer and a small hydrophone detector (Fig. 2), which allowed the fluctuations of the transmitted ultrasonic waves to be measured in a single coherence area or speckle [3]. We used a pulsed technique, for which the ultrasonic field that is typically transmitted through the

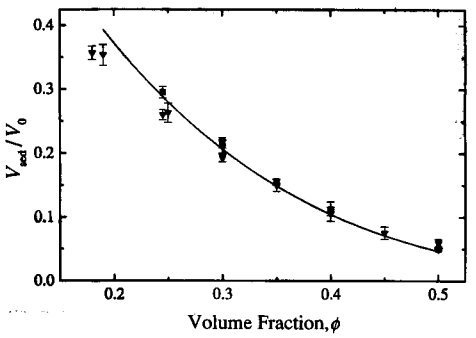

Fig. 1. Sedimentation velocity, normalized by the Stokes velocity V_0, as a function of volume fraction for 0.44-mm-radius glass spheres in a fluid mixture of 75% glycerol and 25% water. The data were measured for two sample thicknessess, $L = 7.76$ mm and 12.2 mm, shown by the triangles and squares, respectively.

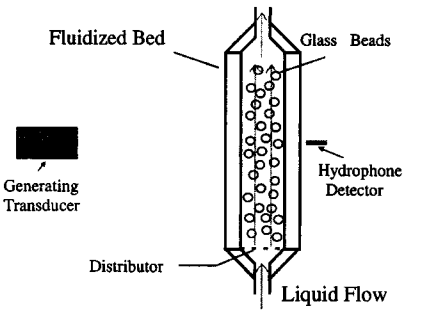

Fig. 2. Schematic diagram of the fluidized bed and transducer arrangement.

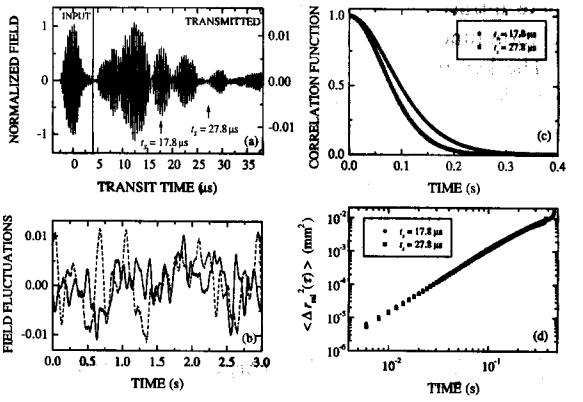

Fig. 3. Typical results in pulsed diffusing wave spectroscopy. (a) Transmitted ultrasonic field in a single speckle (solid curve) compared with the input pulse shown on the left. (b) Field fluctuations at the two sampling times $t_s = 17.8$ μs (dashed curve) and $t_s = 27.8$ μs (solid curve) in the diffusion profile. These field fluctuations were recorded at the pulse repetition rate, so that the time interval between consecutive points in the figure is the pulse repetition period, which was 2 ms in this case. (c) Temporal auto-correlation function of the field fluctuations at these two sampling times. (d) Relative mean square displacement of the particles as a function of time.

sample following the arrival of a single input pulse is illustrated in Fig. 3(a). At this frequency, where $\lambda \sim a$, strong multiple scattering of ultrasound is demonstrated by the fact that the transmitted field extends over a much longer time interval than the input pulse width, as the ultrasound follows progressively longer and longer scattering paths through the sample. On subsequent repetitions of the input pulse, the field fluctuations due to the motion of the particles were measured at a fixed sampling time t_s, corresponding to a path length $s = v_e t_s$, where v_e is the energy velocity of diffusing ultrasound; two representative sampling times are illustrated by the vertical arrows in Fig. 3(a). A short segment of the measured

field fluctuations $F(t)$ at these two sampling times is shown in Fig. 3(b); careful inspection of this figure reveals that the field appears to fluctuate more rapidly at the later sampling time. This is shown more clearly by the temporal field auto-correlation function, $g_1(\tau) = \langle F^*(t)F(t+\tau)\rangle/\langle F^2\rangle$, which we calculate from digitized records of the field fluctuations using a fast Fourier transform method. The results of this calculation are shown in Fig. 3(c), where a significantly more rapid decay of the correlation function measured at the later sampling time is clearly seen. For the data shown in Fig. 3, a sequence of 131 000 pulses was used, allowing us to follow the variation in the field $F(t)$ over approximately 2 min. This was then repeated 50 times, and the temporal auto-correlation functions were averaged together, resulting in accurate measurements of $g_1(\tau)$. Note that these ultrasonic measurements give the field auto-correlation function directly.

The key to determining the motion of the scattering particles from $g_1(\tau)$ in pulsed DAWS is to relate the change in their displacements to the total phase change of the ultrasonic field for multiple scattering paths that reach the detector at t_s [13]. These paths contain $n = s/l^*$ scattering events, where l^* is the transport mean free path of the multiply scattered sound, or the distance traveled before its propagation direction is randomized. For a path of order n, the total phase change is given by

$$\Delta\phi^{(n)}(\tau) = \sum_p^n \Delta\phi_p(\tau) = \sum_p^n [\boldsymbol{k}_p \cdot (\Delta\boldsymbol{r}_{p+1}(\tau) - \Delta\boldsymbol{r}_p(\tau))],$$

where $\boldsymbol{k}_p$ is the wave vector of the wave scattered from the pth to the $(p+1)$th particle in the path, and $\Delta\boldsymbol{r}_{\mathrm{rel},p}(\tau) = \Delta\boldsymbol{r}_{p+1}(\tau) - \Delta\boldsymbol{r}_p(\tau)$ is their relative displacement during the time interval τ [14]. Writing $\Delta\boldsymbol{r}(\tau) = \boldsymbol{u}(\tau)$ and expanding $\Delta\boldsymbol{r}_{\mathrm{rel}}$ to leading order in the separation between adjacent scatterers, $\Lambda_p = |\boldsymbol{r}_{p+1} - \boldsymbol{r}_p|$, we obtain $\Delta\boldsymbol{r}_{\mathrm{rel},p} \approx \Lambda_p(\hat{\boldsymbol{e}}_p \cdot \nabla)\boldsymbol{u}$, where $\hat{\boldsymbol{e}}_p = e_x^{(p)}\hat{\boldsymbol{i}} + e_y^{(p)}\hat{\boldsymbol{j}} + e_z^{(p)}\hat{\boldsymbol{k}}$ is a unit vector in the direction of $\boldsymbol{k}_p$. This allows us to write the phase change $\Delta\phi_p(\tau)$ in terms of the strain tensor

$$\varepsilon_{ij}(\tau) = \tfrac{1}{2}(\partial_i u_j(\tau) + \partial_j u_i(\tau))$$

$$\text{as } \Delta\phi_p(\tau) = k\Lambda_p \sum_{i,j} e_i^{(p)} e_j^{(p)} \varepsilon_{ij}(\boldsymbol{r}_p, \tau).$$

The correlation function is then given by

$$\begin{aligned} g_1(\tau) &= \langle \exp[-i\Delta\phi^{(n)}(\tau)]\rangle \\ &\approx \exp[-sl^*k^2\bar{\varepsilon}^2/6] \\ &\approx \exp[-(s/l^*)k^2\langle\Delta r_{\mathrm{rel}}^2(\tau)\rangle/6], \end{aligned} \quad (1)$$

where $\bar{\varepsilon}$ is the average strain defined by the expression $\bar{\varepsilon}^2 = \frac{2}{5}[\langle(\sum\varepsilon_{ii})^2\rangle + 2\sum_{i,j}\langle\varepsilon_{ij}^2\rangle]$, and $\langle\cdots\rangle$ indicates ensemble average. For fluidized suspensions where the spatial correlations of the particles have short lifetimes, making the correlations difficult to see by eye, it is an excellent approximation to take $\bar{\varepsilon}^2 \approx \langle\Delta r_{\mathrm{rel}}^2(\tau)\rangle/l^{*2}$, so that the decay of the correlation function is determined by the time-dependent mean square displacement of the particles relative to their neighbours located on average a distance l^* away [13]. This simple interpretation also follows from the fact that the quantity measured directly in DAWS is the variance in the change in separation between adjacent particles in the scattering paths.

We determine k, v_e and l^* from measurements of the ballistic and diffusive transport of ultrasound through the suspension [3,5,15,16], enabling the time dependence of $\langle\Delta r_{\mathrm{rel}}^2(\tau)\rangle$ and $\bar{\varepsilon}$ to be determined from the measured correlation functions by inverting Eq. (1). Fig. 3(d) shows our results for the data taken at the two different sampling times in Figs. 3(b) and (c), demonstrating that these data give essentially the same values of $\langle\Delta r_{\mathrm{rel}}^2(\tau)\rangle$. Thus, the dependence of the correlation function on path length is correctly described by Eq. (1), giving confidence in our method of analysis. Data for $\langle\Delta r_{\mathrm{rel}}^2(\tau)\rangle$ at a range of volume fractions are shown in Fig. 4. At early times, the particles move ballistically with a range of different velocities and $\langle\Delta r_{\mathrm{rel}}^2(\tau)\rangle = \langle\Delta V_{\mathrm{rel}}^2\rangle\tau^2$, so that $\langle\Delta r_{\mathrm{rel}}^2(\tau)\rangle$ gives a measure of the local variance in the relative velocity of the particles. In this regime, the strain is also proportional to τ, so DAWS also measures the average local strain rate $\bar{\Gamma} = \bar{\varepsilon}/\tau \approx \Delta V_{\mathrm{rel}}/l^*$, where $\Delta V_{\mathrm{rel}} = \sqrt{\langle\Delta V_{\mathrm{rel}}^2\rangle}$. At later times, $\langle\Delta r_{\mathrm{rel}}^2(\tau)\rangle$ and $\bar{\varepsilon}$ increase less rapidly with time, as the particle trajectories become modified by interactions with their neighbours, allowing us to determine the local crossover time τ_Δ from fits to the phenomenological expression [13] $\langle\Delta r_{\mathrm{rel}}^2(\tau)\rangle = \langle\Delta V_{\mathrm{rel}}^2\rangle\tau^2/[1 + (\tau/\tau_\Delta)^{2-m}]$. Note that in the strong scattering regime where $\lambda \sim a$, l^* is so short that it is approximately equal to the inter-particle spacing throughout the range of the volume fractions studied here; thus, DAWS

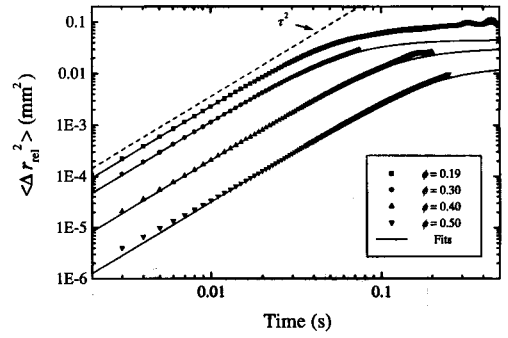

Fig. 4. Relative mean square displacement of the particles as a function of time for several volume fractions ϕ. The solid curves are fits to the phenomenological expression given in the text, allowing both $\langle\Delta V_{\mathrm{rel}}^2\rangle$ and the crossover time τ_Δ to be determined. Note that we find $m = 0$ in this expression, as can easily be seen from the data at the lowest volume fraction, so that the relative particle motion does not cross over to diffusive behaviour on this time scale.

can probe the relative motion of nearest-neighbour particles in the suspension. To probe the local fluctuations at longer length scales, we repeat the experiments at lower frequencies, where l^* becomes larger as the weaker Rayleigh scattering regime is approached. We find a marked increase in the velocity fluctuations with length scale, with $\Delta V_{rel} \propto \sqrt{l^*}$, as l^* is increased by more than a factor of 5, indicating that the spatial correlations of the local velocity fluctuations, previously only seen at very low Re [8], persist at the higher Re investigated in our experiments.

At the length scale of the inter-particle spacing, the volume fraction dependence of ΔV_{rel} and $\bar{\Gamma}$ is shown in Fig. 5, where ΔV_{rel} is normalized by the sedimentation velocity V_{sed}, and $\bar{\Gamma}$ by the sedimentation time a/V_{sed}. Both ΔV_{rel} and $\bar{\Gamma}$ are remarkably large, providing a quantitative measure of the magnitude of the local fluctuations at this very short length scale. ΔV_{rel} exhibits only a weak dependence on ϕ, increasing approximately as $\phi^{1/3}$ at low ϕ, and then decreasing for $\phi > 0.4$, indicating that the local flows become more correlated at the highest ϕ. The ϕ-dependence of $\bar{\Gamma}$ is qualitatively similar, but more pronounced, as at low ϕ we find $\bar{\Gamma} \propto \phi^{2/3}$.

Also shown by crosses in Fig. 5(b) are light scattering results for the strain rate measured at much lower Re and larger length scales [17], raising the question of whether Re or length scale is primarily responsible for the large differences found. Although we have not used DAWS to measure ΔV_{rel} and $\bar{\Gamma}$ at large enough l^* to answer this question directly, we have been able to address this question by applying another novel ultrasonic technique, dynamic sound scattering in the single scattering limit, to measure the rms velocity V_{rms} of the particles [13]. Since $\sqrt{2}V_{rms}$ sets the upper bound that cuts off the growth of ΔV_{rel} with length scale, it allows us to estimate the instantaneous correlation length ξ of the velocity fluctuations at Re $\sim$ 0.3. Thus, we are able to extrapolate $\bar{\Gamma}$ to the same length scales as the low Re measurements, yielding the open symbols in Fig. 5(b); this shows that the values of $\bar{\Gamma}$ at ξ have very little, if any, dependence on Re over this range.

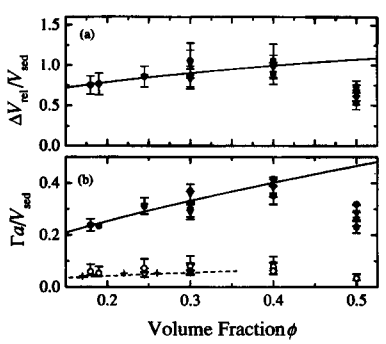

Fig. 5. Volume fraction dependence of the relative velocity fluctuations and strain rate at the length scale of the average inter-particle separation, represented by the solid symbols in (a) and (b), respectively. In (b), the strain rate determined from measurements by Xue et al. [17] at Re $\sim 10^{-4}$ and long length scales is shown by the crosses; these results are compared with our data extrapolated to the length scale of the velocity correlation length ξ, represented by the open symbols.

In summary, our DAWS results provide new information about the velocity fluctuations and strain rate in fluidized suspensions. We find that the behaviour of $\bar{\Gamma}$, V_{rms} and ξ is remarkably similar at Re $\sim$ 0.3 to that found when Re is more than 3 orders of magnitude smaller, a result that should help to discriminate between competing theoretical models. At present, the origin of the velocity correlations in fluidized suspension remains unclear, motivating further DAWS experiments over a wide range of Reynolds numbers and length scales to help elucidate this behaviour.

Acknowledgements

Acknowledgement is made to NSERC, NATO, Imperial Oil Ltd and the donors of the Petroleum Research Fund, administered by the ACS, for support of this research.

References

[1] G. Maret, P.E. Wolf, Z. Phys. B 65 (1987) 409.
[2] D.J. Pine, D.A. Weitz, P.M. Chaikin, E. Herbolzheimer, Phys. Rev. Lett. 60 (1988) 1134.
[3] J.H. Page, H.P. Schriemer, A.E. Bailey, D.A. Weitz, Phys. Rev. E 52 (1995) 3106.
[4] J.H. Page, H.P. Schriemer, I.P. Jones, P. Sheng, D.A. Weitz, Physica A 241 (1997) 64.
[5] H.P. Schriemer, M.L. Cowan, J.H. Page, P. Sheng, Z. Liu, D.A. Weitz, Phys. Rev. Lett. 79 (1997) 3166.
[6] R.E. Caflisch, J.H.C. Luke, Phys. Fluids 28 (1985) 759.
[7] D.L. Koch, E.S.G. Shaqfeh, J. Fluid Mech. 224 (1991) 275.
[8] P.N. Segrè, E. Herbolzheimer, P.M. Chaikin, Phys. Rev. Lett. 79 (1997) 2574.
[9] A. Levine, S. Ramaswamy, E. Frey, R. Bruinsma, Phys. Rev. Lett. 81 (1998) 5944.
[10] T. Tong, B.J. Ackerson, Phys. Rev. E 58 (1998) R6931.
[11] W.B. Russel, D.A. Saville, W.R. Schowalter, Colloidal Dispersions, Cambridge University Press, Cambridge, 1989.
[12] M.L. Cowan, I.P. Jones, J.H. Page, and D.A. Weitz, unpublished.
[13] M.L. Cowan, J.H. Page, D.A. Weitz, unpublished.
[14] D. Bicout, R. Maynard, Physica A 199 (1993) 387.
[15] J.H. Page, P. Sheng, H.P. Schriemer, I. Jones, X. Jing, D.A. Wietz, Science 271 (1996) 634.
[16] M.L. Cowan, K. Beaty, J.H. Page, Z. Liu, P. Sheng, Phys. Rev. E 58 (1998) 6626.
[17] J.-Z. Xue, E. Herbolzheimer, M.A. Rutgers, W.B. Russel, P.M. Chaiken, Phys. Rev. Lett. 69 (1992) 1715.